Icarus xxx (2011) xxx–xxx

Contents lists available at ScienceDirect

Icarus

journal homepage: www.elsevier.com/locate/icarus

Reconciling the centimeter- and millimeter-wavelength ammonia absorption spectra under jovian conditions: Extensive millimeter-wavelength measurements and a consistent model

Kiruthika Devaraj [a,*], Paul G. Steffes [a,1], Bryan M. Karpowicz [b]

[a] School of Electrical and Computer Engineering, Georgia Institute of Technology, 777 Atlantic Drive NW, Atlanta, GA 30332-0250, United States
[b] Atmospheric and Environmental Research, Inc., 131 Hartwell Ave., Lexington, MA 02421, United States

ARTICLE INFO

Article history:
Received 13 August 2010
Revised 3 December 2010
Accepted 10 December 2010
Available online xxxx

Keywords:
Atmospheres, Composition
Jupiter, Atmosphere
Spectroscopy
Experimental techniques

ABSTRACT

Over 1000 laboratory measurements of the 2–4 mm-wavelength opacity of ammonia have been made under simulated jovian atmospheric conditions using a high-precision laboratory system developed at Georgia Tech. These laboratory measurements of the opacity of ammonia were made of various gas mixtures of hydrogen (~77.5–85.5%), helium (~12.5–13.5%), and ammonia (1–10%) at pressures between 1 and 3 bars and temperatures between 200 and 300 K. Laboratory measurements were also made of the opacity of pure ammonia at pressures between 0.05 and 1 bar and temperatures between 200 and 300 K. Using these millimeter-wavelength measurements and close to 2000 cm-wavelength measurements made by Hanley et al. (2009), a new consistent model has been developed to accurately characterize the absorption spectra of ammonia in a hydrogen/helium atmosphere in the 1 mm to 30 cm wavelength range. This model can be used in the 1–30 cm wavelength range at pressures up to 20 bars and temperatures from 200 to 500 K and in the 1 mm to 1 cm wavelength range at pressures up to 3 bars and temperatures from 200 to 300 K. These measurements and the accompanying model will enable better interpretation of the centimeter- and millimeter-wavelength emission spectra of the jovian planets.

1. Introduction

Millimeter-wavelength astronomy is a powerful tool for studying the temperature structure, composition, and dynamics of jovian planetary atmospheres. Furthermore, at millimeter-wavelengths, the planets Uranus and Neptune with small apparent diameters and large flux densities are frequently used as primary calibrators of astronomical sources and telescope parameters (Ulich, 1981; Kramer et al., 2008). To date, ground-based millimeter-wavelength observations have yielded disk-averaged emission measurements of the jovian planets (Ulich, 1974; Griffin et al., 1986; Muhleman and Berge, 1991; Griffin and Orton, 1993; Kramer et al., 2008), interferometric mapping of Saturn (Dowling et al., 1987; van der Tak et al., 1999; Dunn et al., 2005), and interferometric observations of limb darkening of Jupiter (Valdes et al., 1982). Accurate interpretation and modeling of the emission spectra of the jovian planets depend on the knowledge of the atmospheric abundances of various constituents and the opacity of each constituent. The presence of any broad absorption lines in the spectrum of the planet that are not properly accounted for can lead to erroneous predictions of the flux densities. Ammonia is one such constituent known to contribute to strong absorption in the jovian planets and has broad absorption features in the centimeter- and millimeter-wavelength range. Hence, accurate knowledge of the opacity of gaseous ammonia directly impacts the interpretation of the emission spectra of the jovian atmospheres at those wavelengths. Furthermore, since ammonia is one of the predominant centimeter- and millimeter-wavelength absorbers in the jovian planets, its opacity should be known before the potential effects of other absorbing constituents on the emission spectra can be assessed.

The strong absorption of ammonia in the centimeter- and millimeter-wavelength range stems from the presence of a series of strong inversion transitions around 1.25 cm, several strong rotational transitions in the submillimeter region, and a strong ν_2 roto-vibrational transition at 2.15 mm. There has been tremendous interest in understanding the absorption properties of ammonia in the centimeter-wavelength region since they were first measured in the laboratory by Cleeton and Williams (1934). Recently, Hanley et al. (2009) made close to 2000 high-accuracy measurements of the centimeter-wavelength properties of ammonia under simulated jovian atmospheric conditions (pressures up to 12 bars and temperatures up to 450 K) and developed a new model to estimate

* Corresponding author.
E-mail addresses: kdevaraj@ece.gatech.edu (K. Devaraj), steffes@gatech.edu (P.G. Steffes), bkarpowi@aer.com (B.M. Karpowicz).
[1] Fax: +1 404 894 5935.

0019-1035/$ - see front matter © 2010 Elsevier Inc. All rights reserved.
doi:10.1016/j.icarus.2010.12.010

the opacity of ammonia in the centimeter-wavelength range. The millimeter-wavelength absorption properties of pure ammonia were first investigated more than 50 years ago by Nethercot et al. (1952) who measured the absorption of one atmosphere of pure ammonia up to 260 GHz. A few 3.2 mm-wavelength measurements of ammonia gas properties under simulated jovian conditions were made by Joiner and Steffes (1991) and Mohammed and Steffes (2004). However, these millimeter-wavelength measurements had large uncertainties because of the coarse instrumentation used at that time and did not account properly for the adsorption of ammonia on the surface of the test instruments.

Several ammonia absorption models are currently used to estimate the opacity of gaseous ammonia under jovian conditions in the millimeter-wavelength region (Joiner and Steffes, 1991; Mohammed and Steffes, 2003, 2004). These models were derived based on a limited number of millimeter-wavelength measurements and do not accurately represent the absorptivity of ammonia because of limited wavelength ranges measured and the large uncertainties associated with those measurements. There were also difficulties in reconciling the centimeter- and millimeter-wavelength opacity of ammonia (see, e.g., Mohammed and Steffes, 2004). Hence, there has been a strong impetus to make a large number of highly accurate measurements of the millimeter-wavelength properties of ammonia under simulated jovian conditions and to develop a model to estimate the opacity of ammonia in a hydrogen/helium atmosphere over a wide range of pressures, temperatures, and mixing ratios, that is consistent in the centimeter- and millimeter-wavelength range.

Over 700 measurements of the opacity of ammonia in a hydrogen/helium atmosphere at pressures up to 3 bars and temperatures from 200 to 300 K and nearly 300 measurements of the opacity of pure ammonia at pressures up to 1 bar and temperatures from 200 to 300 K have now been made in the 2–4 mm-wavelength range. These millimeter-wavelength measurements and close to 2000 cm-wavelength measurements of the opacity of ammonia made by Hanley et al. (2009) have been used to develop a consistent ammonia opacity model for the reliable interpretation of the ground-based and spacecraft-based observations of the jovian planets in the 1 mm to 30 cm wavelength range. This model can be used in the 1–30 cm wavelength range at pressures up to 20 bars and temperatures from 200 to 500 K and in the 1 mm to 1 cm wavelength range at pressures up to 3 bars and temperatures from 200 to 300 K.

2. Measurement theory and system

The reduction in the quality factor (Q) of a resonant mode of a resonator in the presence of a lossy gas is used to measure the absorption of the gas (see, e.g., Bleaney and Penrose, 1947; Bleaney and Loubser, 1950). The Q is computed as the resonant frequency (f_0) divided by its half-power bandwidth ($HPBW$). When a lossy gas is introduced into the resonator, the resonances broaden due to the opacity of the gas and the center frequency shifts due to the refractivity of the gas mixture. The Q of the resonances of a Fabry–Perot resonator are monitored in the presence of the lossy gas mixture. Subsequently, a non-absorbing or low-loss gas such as argon or carbon dioxide is added to shift the center frequency of the resonances by the same amount as the lossy gas, and dielectrically matched measurements are made. The insertion loss (S) of the resonator is measured in dB at the center frequencies of each resonance and the transmissivities are obtained by $t = 10^{-S/10}$. The formula used for calculating absorptivity is given as (DeBoer and Steffes, 1994)

$$\alpha = 8.686\frac{\pi}{\lambda}\left(\frac{1-\sqrt{t_{loaded}}}{Q^m_{loaded}} - \frac{1-\sqrt{t_{matched}}}{Q^m_{matched}}\right)\ \mathrm{dB/km}, \quad (1)$$

where Q^m_{loaded} and $Q^m_{matched}$ are the measured Qs of the resonances in the loaded and dielectrically matched conditions, respectively, and t_{loaded} and $t_{matched}$ are the transmissivities of the resonances in the loaded and matched conditions, respectively.

The high-sensitivity millimeter-wavelength system used for measuring the opacity of gaseous ammonia under simulated jovian conditions has been described by Devaraj and Steffes (2011). This system operates in the 2–4 mm-wavelength range and consists of a planetary atmospheric simulator, a millimeter-wavelength subsystem (W-band/F-band), and a data handling subsystem. The planetary atmospheric simulator controls and monitors the environment experienced by the measurement system, including the pressure and temperature conditions of the gas under test. The simulator consists of a glass pressure vessel capable of withstanding up to 3 bars of pressure, a temperature chamber capable of operating in the 200–300 K range, gas-handling subsystems, a vacuum pump, and pressure and temperature gauges. The millimeter-wavelength subsystem consists of a W-band system used for measurements in the 3–4 mm-wavelength range and an F-band system used for measurements in the 2–3 mm-wavelength range which is shown in Fig. 1. At the heart of the measurement system is a spherical mirror Fabry–Perot resonator (FPR) that operates in a near confocal configuration and is enclosed in the pressure vessel. The FPR has low losses which correspond to high Qs of between 45,000 and 190,000 at ambient room temperature. The effective path length (EPL) of the electromagnetic energy is given as (Valkenburg and Derr, 1966)

$$\mathrm{EPL} = \frac{Q\lambda}{2\pi}. \quad (2)$$

The EPL for the FPR is between 20 and 120 m, depending on the wavelength and the quality factor of the particular resonance. A swept signal generator (HP 83650B) is used to generate signals which are fed to a times-six active multiplier chain/frequency tripler (Millitech AMC-10-RFH00/Pacific Millimeter Products D3WO) and coupled to the input port of the FPR. The signals from the output port of the FPR are fed to a spectrum analyzer (HP 8564E) via a W-band/F-Band harmonic mixer (QuinStar 922WHP-387/Pacific Millimeter Products DM) and a diplexer (MD1A/MD2A). The data acquisition system consists of a computer connected to the spectrum analyzer (HP 8564E), the swept signal generator (HP 83650B), and a CW signal generator (HP 83712B) via a general purpose interface bus (GPIB). The instruments are controlled via Matlab® and the Standard Commands for Programmable Instruments (SCPI). The software used is similar to that used by Hanley and Steffes (2007) with modifications to account for the suite of instruments used in this measurement system. An elaborate description of the measurement theory and system is given by Devaraj and Steffes (2011).

3. Measurement procedure and uncertainty

The measurement procedure followed in this investigation for characterizing the opacity of polar molecules such as ammonia broadened by non-polar molecules such as hydrogen and helium has been described by Devaraj and Steffes (2011). The measurement process begins by characterizing and selecting standard resonances (TEM_{q00}) with high Q, low asymmetry, and high signal to noise ratio at a particular measurement temperature. Any change in the measurement temperature requires a wait time of several days because of the long thermal time-constant and the necessity to identify the standard resonances at each measurement temperature. Hence, multiple measurements were performed at each temperature using different concentrations of ammonia gas mixture and different pressures. The standard resonances were used to measure the gas opacity for all the measurements performed

Please cite this article in press as: Devaraj, K., et al. Reconciling the centimeter- and millimeter-wavelength ammonia absorption spectra under jovian conditions: Extensive millimeter-wavelength measurements and a consistent model. Icarus (2011), doi:10.1016/j.icarus.2010.12.010

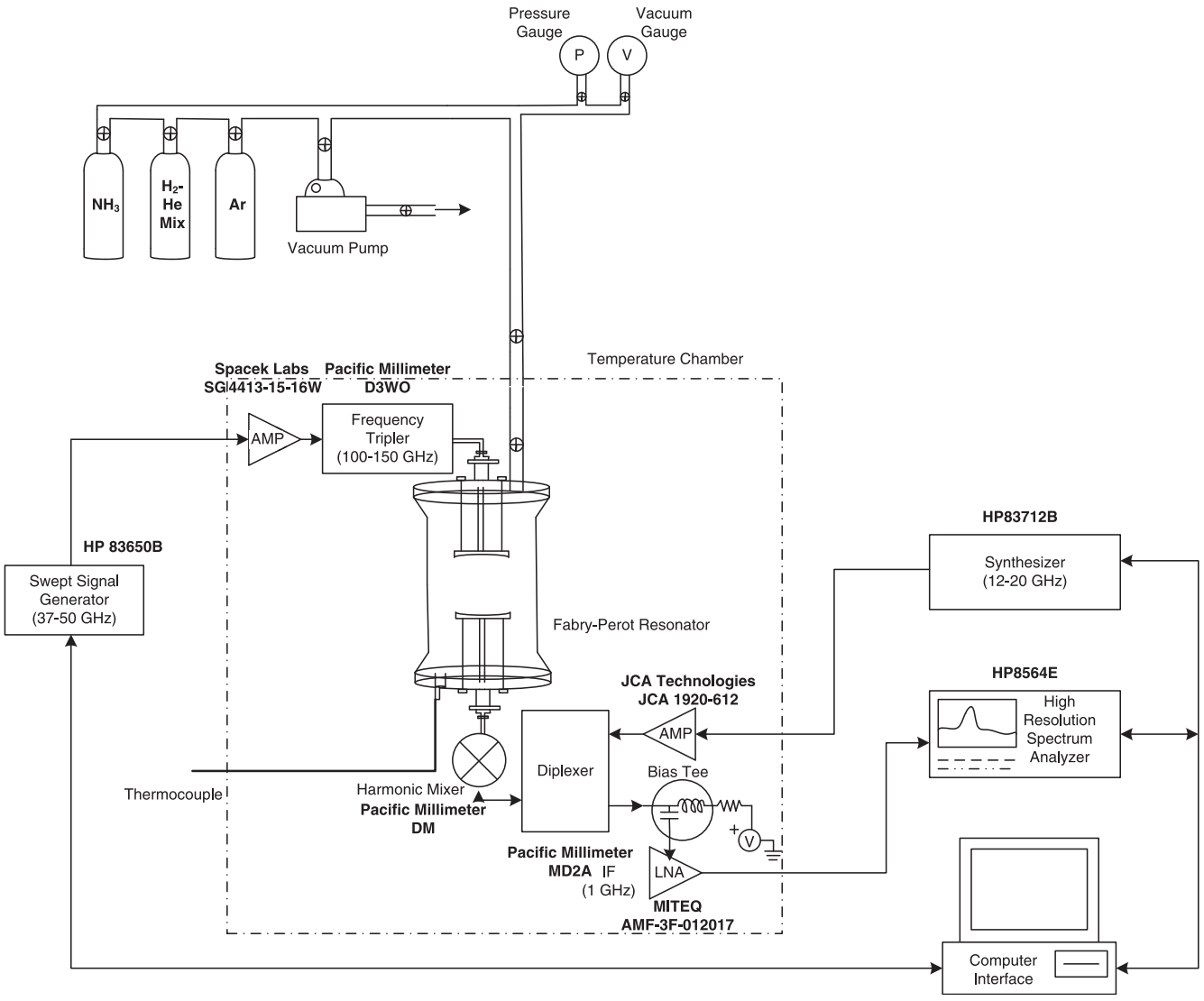

Fig. 1. F-band (2–3 mm) measurement system for studying ammonia gas properties under jovian planetary conditions (Devaraj and Steffes, 2011). Solid lines represent the electrical connections and the arrows show the direction of signal propagation. Valves controlling the flow of gases are shown by the small crossed circles.

at a particular temperature. Whenever ammonia was handled in the system, stringent procedures were exercised to account for the effects of adsorption/desorption of ammonia on the surface of the resonator (Devaraj and Steffes, 2011). Measurements were always performed by first adding ammonia and working up to higher pressures by adding hydrogen/helium to the system. This was done to ensure that there was no additional adsorption/desorption leading to a disproportional change in the concentration of ammonia after the initial adsorption/desorption equilibrium was established.

Each measurement cycle consists of first measuring the resonances of an evacuated resonator. Test gases are then added to the system and the bandwidth and amplitude of the frequency-shifted resonances are measured at different pressures. The system is then vented down to the ambient pressure and a vacuum is drawn to completely remove the test gases and a second set of vacuum measurements of the resonances are made. A non-absorbing or low-loss gas such as argon or carbon dioxide is added to the system to shift the frequency of the resonances by the exact same amount as the test gases and the dielectrically matched measurements are made. The system is evacuated once again to remove the matched gas and a third set of vacuum measurements are made. After this step, the signal generator and detector are disconnected from the resonator and three sets of straight-through transmissivity measurements are made under the same conditions at each pressure/frequency point of the test gas. Three sets of vacuum and straight-through transmissivity measurements are performed to obtain a good statistical characterization of the measurement uncertainties. The data are processed after each measurement cycle is completed. Software written in Matlab® is used to automatically load and process the raw data.

The uncertainties associated with the measurements have been described in detail by Devaraj and Steffes (2011). These uncertainties include instrumental errors (σ_n), errors in dielectric matching (σ_{diel}), transmissivity errors (σ_{trans}), errors due to asymmetry in resonances (σ_{asym}), and errors in measurement conditions (σ_{cond}) arising from uncertainties in the measurement of temperature, pressure and mixing ratio. Instrumental errors arise due to the sensitivity of the electrical devices and their ability to accurately measure the center frequency and bandwidth. Errors in dielectric matching are due to the minor mis-alignments in the center frequency between the loaded and the matched measurements. This is the least significant error because of the highly accurate software-controlled matching of the center frequency between the

Please cite this article in press as: Devaraj, K., et al. Reconciling the centimeter- and millimeter-wavelength ammonia absorption spectra under jovian conditions: Extensive millimeter-wavelength measurements and a consistent model. Icarus (2011), doi:10.1016/j.icarus.2010.12.010

loaded and matched measurements. Transmissivity errors are due to the uncertainties in the measurement amplitude and are caused by the electronics (signal generators/detectors), cables, adapters, and waveguides used in the system. Errors from asymmetry are due to the asymmetric nature of the measured resonances which are caused by the overlapping of the off-axis mode resonances on the axial mode resonances. The measured uncertainties in temperature, pressure, and mixing ratio contribute to the total uncertainties due to measurement conditions (σ_{cond}). Although σ_{cond} does not directly affect the opacity measurements, it still needs to be accounted for while creating accurate models for opacity based on the experimental data.

To illustrate the percentage contribution of different uncertainties to the total 2σ uncertainty of a typical measurement, the different uncertainties for an ambient room temperature ammonia opacity measurement made under simulated jovian conditions are shown in Fig. 2. The dominant factor in the total uncertainty in most cases in the 3–4 mm-wavelength range is σ_n and that in the 2–3 mm-wavelength range is σ_{trans}.

4. Ammonia opacity measurements

Over 1000 high-accuracy measurements of the 2–4 mm-wavelength absorptive properties of pure ammonia and ammonia broadened by hydrogen and helium have been made using the millimeter-wavelength measurement system. Certified ultra-high purity ammonia gas cylinders and premixed hydrogen/helium cylinders from Airgas, Inc. were used for the experiments. In the premixed hydrogen/helium cylinder, helium mixing ratio was (13.6 ± 0.272)% and the remainder was hydrogen. This is approximately the helium mole fraction at Jupiter measured by von Zahn et al. (1998). A total of 718 data points of the opacity of ammonia in a hydrogen/helium environment and 295 data points of the opacity of pure ammonia were measured with each data point uniquely representing a combination of pressure, temperature, mixing ratio, and frequency. Pure ammonia opacity measurements were made to accurately characterize its self-broadening parameters. Table 1 lists the measurements taken along with the experiment dates. The entire set of ammonia opacity measurements is provided in Supplemental material to this paper in electronic format (*mmwavelength_nh3_measurements.dat*).

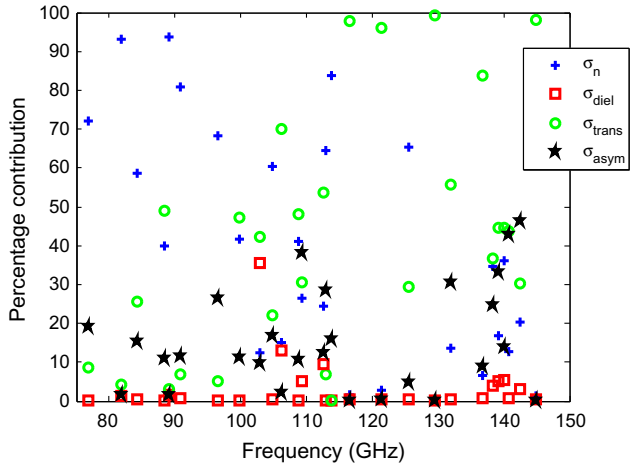

Fig. 2. Percentage contribution of the different measurement uncertainties to the total uncertainty for each resonance at ambient room temperature of the millimeter-wavelength measurement system.

5. Data fitting

The goal of the laboratory measurements described in this paper has been to create a model that accurately estimates the opacity of ammonia under diverse conditions in the frequency/temperature/pressure/concentration (fTPC) space. For the data-fitting process, 1013 Fabry–Perot resonator measurements of the 75–150 GHz opacity of ammonia made by these authors and 1431 cavity resonator measurements of the 1.5–27 GHz opacity of ammonia made by Hanley et al. (2009) were utilized so as to obtain a consistent model in the fTPC space. The 250 Fabry–Perot resonator measurements of the 22–40 GHz opacity of ammonia made by Hanley et al. (2009) were not used in the model development, but instead were used to evaluate the model performance. The method used for data-fitting was a Levenberg–Marquardt optimization technique (Levenberg, 1944; Marquardt, 1963) with a minimization function

$$\chi = \frac{\sqrt{DW} \times (\alpha_{measured} - \alpha_{model})}{\sigma_{measured}}, \quad (3)$$

where DW is the data weight assigned to each data point, $\alpha_{measured}$, α_{model}, and $\sigma_{measured}$ are the measured opacity, modeled opacity of the model under optimization, and measured 2σ uncertainty in opacity, respectively. The sum of squared value of this function was minimized multiple times using random input seed values until a convergent solution was found. The data weight is given as (Hanley et al., 2009)

$$DW = \frac{1}{f_{count}} + \frac{1}{T_{count}} + \frac{1}{P_{count}} + \frac{1}{C_{count}}, \quad (4)$$

where f_{count}, T_{count}, P_{count}, and C_{count} represent the values for the frequency, temperature, pressure, and gas concentration, respectively, of the data points in the four-dimensional *fTPC* space and are listed in Table 2. The approach used divides the data points into roughly equally spaced bins that span the *fTPC* space and each data point is scaled with its data weight so as to prevent the accuracy of the derived model from being skewed toward the most often measured conditions.

The free parameters of the model for ammonia were constrained before those for hydrogen/helium. The pure ammonia measurements were divided into two groups with one group

Table 1
Listing of all experimental conditions for the 2–4 mm-wavelength ammonia opacity measurements performed using the Fabry–Perot resonator as part of this work.

Experiment dates	Temperature range (K)	Pressure range (bars)	NH_3 Mole fraction	Frequency range (GHz)
07/2007–10/2007	295–300	1–3	0.02–0.04	75–120
12/2007–02/2008	218–222	1–3	0.02	75–120
08/2008–09/2008	295–300	1–3	0.02–0.04	110–150
10/2008–11/2009	295–300	0.1–1	1	110–150
11/2008–12/2009	295–300	0.1–1	1	75–120
01/2009–02/2009	218–222	0.1–3	0.02–1	110–150
02/2009–03/2009	218–222	0.1–3	0.02–1	75–120
03/2009–04/2009	203–208	0.1–3	0.02–1	110–150
04/2009–05/2009	203–208	0.1–3	0.02–1	75–120

Please cite this article in press as: Devaraj, K., et al. Reconciling the centimeter- and millimeter-wavelength ammonia absorption spectra under jovian conditions: Extensive millimeter-wavelength measurements and a consistent model. Icarus (2011), doi:10.1016/j.icarus.2010.12.010

Table 2
The breakdown of the ammonia opacity measurements used for data fitting in the fTPC space.

Frequency range (GHz)	f_{count}	Temperature range (K)	T_{count}	Pressure range (bars)	P_{count}	Concentration range (%)	C_{count}
$f < 6$	874	$T < 210$	291	$P < 0.5$	459	$C < 0.5$	380
$6 \leqslant f < 27$	557	$210 \leqslant T < 230$	650	$0.5 \leqslant P < 1$	213	$0.5 \leqslant C < 1$	578
$75 \leqslant f < 100$	329	$230 \leqslant T < 300$	1195	$1 \leqslant P < 2$	533	$1 \leqslant C < 4$	481
$100 \leqslant f < 120$	393	$300 \leqslant T < 380$	112	$2 \leqslant P < 5$	761	$4 \leqslant C < 10$	557
$120 \leqslant f < 150$	291	$380 \leqslant T < 450$	196	$5 \leqslant P \leqslant 12.5$	478	$10 \leqslant C \leqslant 100$	448

constituting the data points with $f \leqslant 100$ GHz (group I) and the other group constituting the data points with $f > 100$ GHz (group II). For the data points in group I, the inversion and rotational transitions of ammonia contribute significantly to the measured opacity and the contribution from the v_2 roto-vibrational transitions is negligible. The v_2 roto-vibrational transitions contribute significantly to the measured opacity when $f > 100$ GHz. Data fitting was achieved for group I by optimizing the ammonia free parameters of the model for the inversion and rotational transitions. After this step, group II data points were used for optimization of the ammonia free parameters of the model for the v_2 transitions. Subsequent optimization steps involved assigning the values obtained from the previous optimization steps to the ammonia free parameters and optimizing only the hydrogen and helium free parameters of the model using the ammonia/hydrogen/helium mixture measurements. The mixture measurements were subdivided into two groups: group III comprising the data points with $f \leqslant 100$ GHz and group IV comprising the data points with $f > 100$ GHz. The hydrogen and helium free parameters of the model for the inversion and rotational transitions were optimized using group III data points and the hydrogen and helium free parameters of the model for the v_2 roto-vibrational transitions were optimized using group IV data points. This procedure was repeated several times with different input seed values for the free parameters, until a convergent solution was obtained. Once the free parameters were constrained, the performance of the new model was assessed by comparing it with the room-temperature measurements of the 22–40 GHz opacity of ammonia made by Hanley et al. (2009) using a Fabry–Perot resonator and found to significantly outperform all the other models.

6. Model development

The impetus for the laboratory measurements is the development of a consistent mathematical formalism to determine the opacity of ammonia under simulated jovian conditions in the centimeter- and millimeter-wavelength range. The new formalism for the hydrogen- and helium-broadened opacity of ammonia estimates the absorptivity at a particular frequency by summing the contribution from the inversion, rotational, and v_2 roto-vibrational transitions listed in the latest JPL spectral line catalog (Pickett et al., 1998) recently updated by Yu et al. (2010c). The references from which the latest JPL spectral line catalog entries were obtained are listed on the JPL website (Yu et al., 2010a,b) and are provided as Supplementary material to this paper (*d017002.pdf* and *d017004.pdf*).

6.1. Absorption formalisms using the JPL line catalog

The absorption from a collisionally broadened gas can be expressed as

$$\alpha = \sum_j A_j \pi \Delta v_j F_j(v, v_{(0,j)}, \ldots) \quad (\mathrm{cm}^{-1}), \tag{5}$$

where for the line j, A_j is the absorption at the line center in cm^{-1}, Δv_j is the linewidth (half width at half max) in cm^{-1}, $F_j(v, v_{0,j}, \ldots)$ is the lineshape function in cm, $v_{(0,j)}$ is the frequency at the line center in cm^{-1}, and v is the frequency of the incident electromagnetic wave in cm^{-1} (see, e.g., Townes and Schawlow, 1955).

The absorption at the line center is calculated using information from the latest JPL catalog as per Pickett et al. (1998)

$$A_j = \frac{n I_j(T)}{\pi \Delta v_j} \quad (\mathrm{cm}^{-1}), \tag{6}$$

where n is the number density of the gas in molecules/cm^3, $I_j(T)$ is the intensity of the line in cm^{-1}/(molecule/cm^2) at temperature T, and with Δv_j expressed in cm^{-1}. Assuming ideal gas behavior, n is calculated as

$$n = \frac{0.1 \times P}{k_B T}, \tag{7}$$

where P is the partial pressure of the gas under consideration in bars, T is the temperature in K, and $k_B = 1.38 \times 10^{-23}$ J/K (Boltzmann's constant). Some caution must be exercised when using the ideal gas assumption under deep jovian conditions because gases are hardly ideal under high pressures (see, e.g., Van der Waals, 1873; Span, 2000). The line intensity at the measurement temperature T is calculated as

$$I_j(T) \approx I_j(T_0) \left(\frac{T_0}{T}\right)^{\eta+1} \exp\left(\left(\tfrac{1}{T_0} - \tfrac{1}{T}\right) E_{(l,j)} (hc/k_B)\right), \tag{8}$$

where $I_j(T_0)$ is the intensity of the line at the reference temperature T_0, $E_{(l,j)}$ is the lower state energy of the transition in cm^{-1}, c is the speed of light in cm/s, h is the Planck's constant in Js, and η is the temperature dependence and is $\approx 3/2$ for non-linear and symmetric-top molecules such as ammonia, and 1 for linear molecules. The values of $v_{(0,j)}$, $I_j(T_0)$, and $E_{(l,j)}$ at the reference temperature can be found in the latest JPL spectral line catalog (Pickett et al., 1998) (*Version 5, September 2010*). The values of $I_j(T_0)$ given in the JPL catalog have units of $\log_{10}(\mathrm{nm}^2\,\mathrm{MHz})$ and must be taken as the exponent of 10 and divided by $2.99793458 \times 10^{18}$ to be converted to cm^{-1}/(molecule/cm^2). The linewidth for a gas mixture is calculated by

$$\Delta v_j = \sum_i \Delta v^o_{(i,j)} P_i \left(\frac{T_0}{T}\right)^{\xi_{ij}} \quad (\mathrm{cm}^{-1}), \tag{9}$$

where for the gas i and line j, $\Delta v^o_{(i,j)}$ is the line broadening parameter in cm^{-1}/bar, P_i is the partial pressure of gas in bars, and ξ_{ij} is the temperature dependence of the line broadening parameter. The temperature dependence is calculated as (e.g., DeBoer and Steffes, 1994)

$$\Delta v_j \propto T^{-(m+1)/2(m-1)} = T^{-\xi}, \tag{10}$$

where $1 < m < \infty$. For neutral gases, $m = 3$ is a lower limit and hence $0.5 < \xi < 1.0$.

6.2. Lineshapes

Under the pressure and temperature conditions used for our measurements, the greatest source of line broadening is from molecular collisions. These collisions allow for the transfer of

Please cite this article in press as: Devaraj, K., et al. Reconciling the centimeter- and millimeter-wavelength ammonia absorption spectra under jovian conditions: Extensive millimeter-wavelength measurements and a consistent model. Icarus (2011), doi:10.1016/j.icarus.2010.12.010

kinetic energy and interactions between the molecules due to van der Waals force. Lorentz (1906) was the first to model the pressure broadening of gases, with his work focusing on optical wavelength. Debye (1929) described the absorption and refraction in polar molecules with a theory that differed from that of Lorentz at the zero resonant frequency. Van Vleck and Weisskopf (1945) combined the two theories to derive the Van Vleck–Weisskopf lineshape given as

$$F_{VVW}(\nu,\nu_{(0,j)},\Delta\nu_j)=\frac{1}{\pi}\left(\frac{\nu}{\nu_{(0,j)}}\right)^2\left[\frac{\Delta\nu_j}{(\nu_{(0,j)}-\nu)^2+\Delta\nu_j^2}+\frac{\Delta\nu_j}{(\nu_{(0,j)}+\nu)^2+\Delta\nu_j^2}\right], \tag{11}$$

where for the line j, $\Delta\nu_j$ is the half width at half-maximum, $\nu_{(0,j)}$ is the center frequency of the line transition, and ν is the frequency of the incident electromagnetic wave. Gross (1955) assumed a Maxwellian distribution of molecular velocities, instead of the Boltzmann one used by Lorentz and Van Vleck and Weisskopf and derived the Gross or the Kinetic lineshape given by

$$F_G(\nu,\nu_{(0,j)})=\frac{1}{\pi}\left(\frac{\nu}{\nu_{(0,j)}}\right)\left[\frac{4\nu\nu_{(0,j)}\Delta\nu_j}{(\nu_{(0,j)}^2-\nu^2)^2+4\nu^2\Delta\nu_j^2}\right]. \tag{12}$$

Although the Van Vleck–Weisskopf and Gross lineshapes converge at the line center, the Gross lineshape has higher skirts away from the line center than the Van Vleck–Weisskopf lineshape. Ben-Reuven (1966) derived a lineshape with two additional parameters, a line shift term (δ) proportional to the gas density, and a line-to-line coupling element (ζ). The Ben–Reuven lineshape is given by

$$F_{BR}(\nu,\nu_{(0,j)},\gamma_j,\zeta_j,\delta_j)=\frac{2}{\pi}\left(\frac{\nu}{\nu_{(0,j)}}\right)^2\times\left[\frac{(\gamma_j-\zeta_j)\nu^2+(\gamma_j+\zeta_j)\left[(\nu_{(0,j)}+\delta_j)^2+\gamma_j^2-\zeta_j^2\right]}{\left[\nu^2-(\nu_{(0,j)}+\delta_j)^2-\gamma_j^2+\zeta_j^2\right]^2+4\nu^2\gamma_j^2}\right], \tag{13}$$

where for the line j, $\gamma_j=\Delta\nu_j$ is the linewidth. The Gross lineshape is a special case of the Ben–Reuven lineshape under the assumption that only sense-reversing collisions take place, in which case $\gamma_j=\zeta_j$ and $\delta=0$ (Waters, 1976).

6.3. Line parameters

The JPL spectral line catalogs for NH_3 and $NH_3-\nu_2$ have been recently updated (see, e.g., Yu et al., 2010c) and the line transitions in the 0.3–1300 GHz frequency range and their intensities are shown in Fig. 3. The NH_3 catalog has a total of 1716 transitions that include 415 inversion transitions in the 0.3–220 GHz frequency range and 1301 rotational transitions in the 0.3–20 THz frequency range. The $NH_3-\nu_2$ catalog has a total of 4198 roto-vibrational transitions in the 0.02–46 THz frequency range. A total of 5914 transitions are used in the latest opacity formalism for ammonia.

For the development of the new ammonia opacity model described in this paper, different lineshapes were investigated in order to obtain the best fit for the measurements. By using a modified Ben-Reuven (1966) lineshape for the inversion transitions, and a modified Gross (1955) lineshape for the rotational and ν_2 roto-vibrational transitions, it was possible to achieve a robust fit for the measurements. The lineshapes rely on the knowledge of the linewidths of the gases being studied. Laboratory measurements of the self and foreign gas broadening parameters of various line transitions were used where those data were available. When laboratory measurements of the broadening parameters were not available, those parameters were made free variables in the optimization process and the values closest to the average of the available measured broadening parameters that best fit the opacity measurements described in this paper were used.

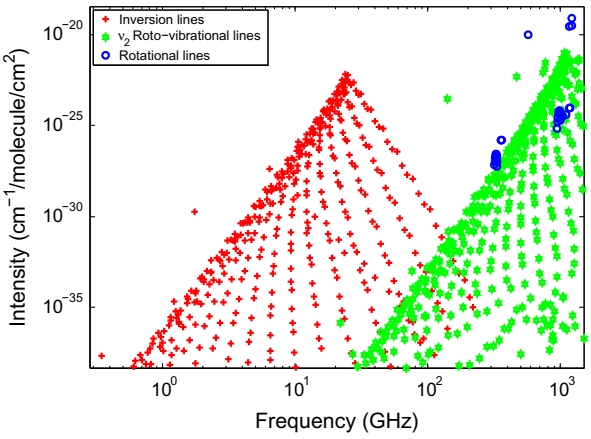

Fig. 3. Line positions and intensities of the NH_3 transitions from 0.3 to 1300 GHz.

6.4. Ammonia opacity formalism

The new model for the hydrogen- and helium-broadened opacity of ammonia uses a modified Ben–Reuven lineshape for the inversion transitions and a modified Gross lineshape for the rotational and ν_2 roto-vibrational transitions. The cumulative opacity is calculated by

$$\alpha=(\alpha_{inv}+\alpha_{rot}+\alpha_{\nu_2})\times 434294.5 \quad (\mathrm{dB/km}), \tag{14}$$

where α_{inv}, α_{rot}, and α_{ν_2} are the opacities from the inversion, rotational, and ν_2 transitions, respectively, in cm^{-1}. The multiplication factor of 434294.5 converts the total opacity from cm^{-1} to dB/km.

The opacity from the inversion transitions is calculated using a modified Ben–Reuven lineshape in a fashion similar to that described by Hanley et al. (2009) but with a different set of values for the model constants than those used by Hanley. The model constants were obtained by optimizing the free parameters of the model to fit the centimeter- and millimeter-wavelength measurements. The opacity from the inversion lines is given as

$$\alpha_{inv}=\frac{0.1D_{inv}P_{NH_3}}{k_BT}\left(\frac{2}{\pi}\right)\left(\frac{T_0}{T}\right)^{\eta+1}\times\sum_j\left(I_j(T_0)\exp\left(\left(\tfrac{1}{T_0}-\tfrac{1}{T}\right)E_{(1,j)}\left(\tfrac{hc}{k_B}\right)\right)\left(\frac{\nu}{\nu_{(0,j)}}\right)^2\times\left[\frac{(\gamma_j-\zeta_j)\nu^2+(\gamma_j+\zeta_j)\left[(\nu_{(0,j)}+\delta_j)^2+\gamma_j^2-\zeta_j^2\right]}{\left[\nu^2-(\nu_{(0,j)}+\delta_j)^2-\gamma_j^2+\zeta_j^2\right]^2+4\nu^2\gamma_j^2}\right]\right) \quad (\mathrm{cm^{-1}}), \tag{15}$$

where for the inversion line j, $\nu_{(0,j)}$, γ_j, ζ_j, and δ_j are the center frequency, linewidth, coupling parameter, and shift parameter, respectively, in cm^{-1}, and D_{inv} is a unitless scale factor. The frequency, linewidth, coupling, and shift parameters are nominally expressed in GHz and should be converted to cm^{-1} before they are used in the equation for opacity. The linewidth and the coupling parameter of the lines are calculated by summing the contribution from different gases and are given by

$$\gamma_j=\gamma_{H_2}P_{H_2}\left(\frac{300}{T}\right)^{\Gamma_{H_2}}+\gamma_{He}P_{He}\left(\frac{300}{T}\right)^{\Gamma_{He}}+\gamma_{NH_3}\gamma_{(0,j)}P_{NH_3}\left(\frac{295}{T}\right)^{\Gamma_{NH_3}} \quad (\mathrm{GHz}), \tag{16}$$

Please cite this article in press as: Devaraj, K., et al. Reconciling the centimeter- and millimeter-wavelength ammonia absorption spectra under jovian conditions: Extensive millimeter-wavelength measurements and a consistent model. Icarus (2011), doi:10.1016/j.icarus.2010.12.010

$$\zeta_j = \zeta_{H_2} P_{H_2} \left(\frac{300}{T}\right)^{Z_{H_2}} + \zeta_{He} P_{He} \left(\frac{300}{T}\right)^{Z_{He}} + \zeta_{NH_3} \gamma_{(0,j)} P_{NH_3} \left(\frac{295}{T}\right)^{Z_{NH_3}} \quad (\text{GHz}), \tag{17}$$

where for the inversion line j and $i = H_2$, He, and NH_3, γ_i and ζ_i are constant scale terms, and Γ_i and Z_i represent the constant temperature dependences of the broadening of each of the gases, P_i are the partial pressures in bar, and $\gamma_{(0,j)}$ are the self-broadening linewidths of the inversion transitions of ammonia in MHz/Torr. The values for $\gamma_{(0,j)}$ are from the calculations of Poynter and Kakar (1975) assuming a T_0 of 295 K. For the lines with center frequencies below 7.2 GHz and $J > 16$, where J represents the total angular momentum vector of the ammonia molecule, γ_0 is expressed as

$$\gamma_0(J,K) = 25.923 \frac{K}{\sqrt{J(J+1)}} \quad (\text{MHz/Torr}), \tag{18}$$

where K is the projection of J onto the axis of symmetry that passes from the center of the nitrogen atom through the point of equidistance in the hydrogen plane of the ammonia molecule. The $\gamma_{(0,j)}$ of all the other inversion lines which are not listed by Poynter and Kakar (1975) and whose $J < 16$ or center frequency >7.2 GHz are assigned a constant value equal to the average of the γ_0 of the lines calculated by Poynter and Kakar. The pressure shift parameter is calculated by

$$\delta_j = d \times \gamma_j \quad (\text{GHz}), \tag{19}$$

where d is an empirically derived constant. All the inversion transitions are assigned the same model constants, even though each line transition behaves differently (see, e.g., Hanley et al., 2009). The equation for computing the opacity of the inversion transitions has 14 free parameters that must be either determined theoretically or empirically. Some of the free parameters were assigned the same values used by Hanley et al. (2009). Since the broadening effects of hydrogen and helium were not measured separately, theoretical values were assigned for the helium model constants. The exponents Γ_{He} and Z_{He} were assigned the theoretical value of 2/3 and the scale factors γ_{He} and ζ_{He} were assigned the values used by Berge and Gulkis (1976), 0.75 and 0.3, respectively. The exponent Γ_{NH_3} was assigned a theoretical value of 1. The other model constants were empirically derived by data-fitting and are listed in Table 3. The units of γ_0 remain in MHz/Torr and the conversion to GHz/bar is incorporated in the scale terms γ_{NH_3} and ζ_{NH_3}.

The opacity from the rotational transitions is calculated using a modified Gross lineshape and is given as

$$\alpha_{rot} = \frac{0.1 D_{rot} P_{NH_3}}{k_B T} \left(\frac{1}{\pi}\right) \left(\frac{T_0}{T}\right)^{\eta+1} \times \sum_j \left[I_j(T_0) \exp\left(\left(\frac{1}{T_0} - \frac{1}{T}\right) E_{(l,j)} \left(\frac{hc}{k_B}\right) \right) \left(\frac{\nu}{\nu_{(0,j)}}\right) \cdot \left(\frac{4\nu\nu_{(0,j)}\Delta\nu_j}{\left(\nu_{(0,j)}^2 - \nu^2\right)^2 + 4\nu^2\Delta\nu_j^2} \right) \right] \quad (\text{cm}^{-1}), \tag{20}$$

where for the rotational line j, $\nu_{(0,j)}$ is the frequency of transition, $\Delta\nu_j$ is the linewidth parameter, and D_{rot} is an empirically derived unitless scale factor. The linewidth parameter is given as

$$\Delta\nu_j = c_{H_2} \Delta\nu_{(H_2,j)} P_{H_2} \left(\frac{300}{T}\right)^{\xi_{H_2}} + c_{He} \Delta\nu_{(He,j)} P_{He} \left(\frac{300}{T}\right)^{\xi_{He}} + c_{NH_3} \Delta\nu_{(NH_3,j)} P_{NH_3} \left(\frac{300}{T}\right)^{\xi_{NH_3}} \quad (\text{GHz}), \tag{21}$$

where for $i = H_2$, He, and NH_3, c_i and ξ_i are the empirically derived model constants, and $\Delta\nu_{(i,j)}$ are the broadening parameters. The units of $\Delta\nu_j$ should be converted from GHz to cm^{-1} before it is used in the equation for computing the opacity from the rotational lines. The self-broadened linewidth for the $J = 1 \leftarrow 0$ transition of the ammonia molecule is assigned the value measured by Belov et al. (1983), and the hydrogen- and helium-broadened linewidths for the $J = 1 \leftarrow 0$ transition are assigned values measured by Bachet (1973). The self- and H_2-broadened linewidths for each of the other rotational lines are assigned values measured by Brown and Peterson (1994). The linewidths for the lines that were not measured by Brown and Peterson were assigned values computed using their extrapolation formula. The He-broadened linewidths are assigned the values computed using the formula given by Pine et al. (1993). The empirically derived model constants for the rotational transitions are listed in Table 4.

Table 3
Values of the model constants used for computing the H_2/He-broadened NH_3 absorptivity from the inversion transitions of the new model.

	$i = H_2$	$i = He$	$i = NH_3$
γ_i	1.7947	0.75	0.7719
Γ_i	0.8357	2/3	1
ζ_i	1.2031	0.3	0.5620
Z_i	0.8610	2/3	0.6206
d		−0.0404	
D_{inv}		0.9903	

The opacity from the ν_2 roto-vibrational transitions is calculated using a modified Gross lineshape and is given as

$$\alpha_{\nu_2} = \frac{0.1 D_{\nu_2} P_{NH_3}}{k_B T} \left(\frac{1}{\pi}\right) \left(\frac{T_0}{T}\right)^{\eta+1} \times \sum_j \left[I_j(T_0) \exp\left(\left(\frac{1}{T_0} - \frac{1}{T}\right) E_{(l,j)} \left(\frac{hc}{k_B}\right) \right) \left(\frac{\nu}{\nu_{(0,j)}}\right) \times \left(\frac{4\nu\nu_{(0,j)}\Delta\nu}{\left(\nu_{(0,j)}^2 - \nu^2\right)^2 + 4\nu^2\Delta\nu^2} \right) \right] \quad (\text{cm}^{-1}), \tag{22}$$

where for the ν_2 roto-vibrational line j, $\nu_{(0,j)}$ is the frequency of transition, $\Delta\nu$ is the linewidth parameter, and D_{ν_2} is an empirically derived unitless scale factor. The linewidth parameter is given by

$$\Delta\nu = \Delta\nu_{H_2} P_{H_2} \left(\frac{300}{T}\right)^{\xi_{H_2}} + \Delta\nu_{He} P_{He} \left(\frac{300}{T}\right)^{\xi_{He}} + \Delta\nu_{NH_3} P_{NH_3} \left(\frac{300}{T}\right)^{\xi_{NH_3}} \quad (\text{GHz}), \tag{23}$$

where for $i = H_2$, He, and NH_3, ξ_i are the empirically derived temperature coefficients, and $\Delta\nu_i$ are the empirically derived broadening parameters for the ν_2 transitions and are listed in Table 5. The units of $\Delta\nu$ should be converted from GHz to cm^{-1} before it is used in the equation for computing the opacity. The self-broadening parameter of the strongest ν_2 transition in the millimeter-wavelength region ($\nu_0 = 140.143$ GHz) was theoretically calculated by Belli et al. (1997). However, the theoretically calculated value of 13.72 GHz/bar was too large to fit the opacity measurements. The self-broadening parameter of the 466 GHz ν_2 transition was measured by

Table 4
Values of the model constants used for computing the H_2/He-broadened NH_3 absorptivity from the rotational transitions of the new model.

	$i = H_2$	$i = He$	$i = NH_3$
c_i	0.2984	0.75	3.1789
ξ_i	0.8730	2/3	1
D_{rot}		2.4268	

Please cite this article in press as: Devaraj, K., et al. Reconciling the centimeter- and millimeter-wavelength ammonia absorption spectra under jovian conditions: Extensive millimeter-wavelength measurements and a consistent model. Icarus (2011), doi:10.1016/j.icarus.2010.12.010

Table 5
Values of the model constants used for computing the H_2/He-broadened NH_3 absorptivity from the ν_2 roto-vibrational transitions of the new model.

	$i = H_2$	i = He	$i = NH_3$
$\Delta\nu_i$ (GHz/bar)	1.4	0.68	9.5
ξ_i	0.73	0.5716	1
D_{ν_2}		1.1206	

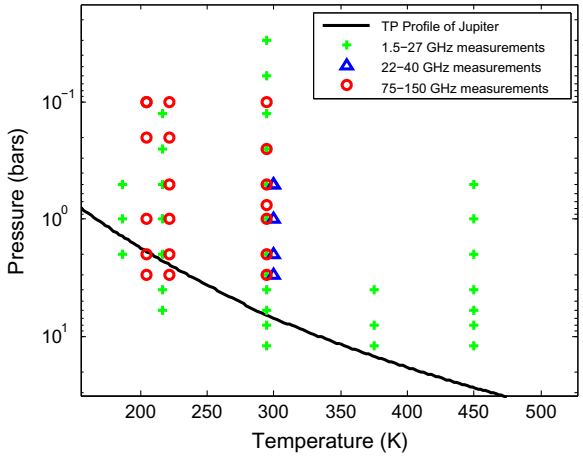

Fig. 4. Dry jovian adiabatic temperature–pressure (*TP*) profile along with the *TP* space measurement points used in the evaluation of the new model performance. Green pluses are the 1.5–27 GHz cavity resonator *TP* space points measured by Hanley et al. (2009), blue triangles are the 22–40 GHz Fabry–Perot resonator *TP* space points measured by Hanley et al. (2009), and red circles are the 75–150 GHz Fabry–Perot *TP* space measurement points described in this paper. (For interpretation of the references to color in this figure legend, the reader is referred to the web version of this article.)

Belov et al. (1982). The self-, hydrogen-, and helium-broadening parameters of most of the ν_2 transitions have not been measured. Hence, the broadening parameters were made free variables during model optimization and empirically derived constant values are used for all lines.

The values of the model constants listed in this paper were optimized to the latest JPL spectral line catalogs (Pickett et al., 1998) (Version 5, September 2010). The frequency, line intensity, and lower state energy of the various transitions of ammonia given in the latest JPL catalogs along with the self- and hydrogen-/helium-broadening parameters for these transitions are provided as Supplementary material to this paper (*ammonia_inversion.dat*, *ammonia_rotational.dat*, and *ammonia_rotovibrational.dat*). Software for running the model in Matlab® is also provided as a supplement (*nh3devarajsteffesmodel.m*). This model can be used to estimate the opacity of ammonia under jovian conditions in the centimeter-wavelength range at pressures up to 20 bars and temperatures in the 200–500 K range and in the millimeter-wavelength range at pressures up to 3 bars and temperatures in the 200–300 K range. This model cannot be used to estimate the opacity of ammonia under deep jovian conditions since the model parameters were not optimized to perform under those conditions and also because the ideal gas assumption used to calculate the opacity does not hold under high pressures.

7. Model performance

Assessing the performance of the model with respect to the measured data provides insights into the goodness of fit of the model and the conditions of its effectiveness. The model was compared with 1431 data points measured by Hanley et al. (2009) of the 1.5–27 GHz opacity of ammonia taken using cylindrical cavity resonators and 250 data points measured by Hanley et al. (2009) of the 22–40 GHz opacity of ammonia taken using a Ka-band Fabry–Perot resonator, in addition to the 1013 data points of the 75–150 GHz opacity of ammonia described in this paper. A possibly dry jovian adiabatic temperature-pressure profile overlayed with the temperature-pressure measurement points used for the model evaluation is shown in Fig. 4.

The new ammonia opacity model fits 66.44% of the 75–150 GHz measurements, 95.11% of the 1.5-27 GHz cavity resonator measurements, and 94.8% of the 22–40 GHz Ka-band Fabry–Perot resonator measurements within 2σ uncertainty. Overall, the model fits 84.3% of the 2694 measurements in the 1.5–150 GHz range within 2σ uncertainty. Comparison of the new model performance with the models of Berge and Gulkis (1976), Spilker (1990), Joiner and Steffes (1991), Mohammed and Steffes (2003, 2004), and Hanley et al. (2009) is listed in Table 6. Plots comparing some of the measured data to the models are shown in Figs. 5–12. The error bars shown in the plots are the 2σ measurement uncertainties. The Mohammed and Steffes (2003) model is only applicable in the Ka-band region and hence only shown in Fig. 6, and the Mohammed and Steffes (2004) model is only applicable in the W-band region and hence only shown in Figs. 7–12. In the implementation of the model by Joiner and Steffes (1991), there were difficulties in matching the numerical values given by the author. Hanley et al. (2009) describe similar difficulties in reproducing the original numerical values given by Joiner and Steffes (1991). However, the numerical values estimated by Hanley et al. (2009) for the various models are consistent with the values estimated by these authors. An example of the opacity of ammonia computed using the new model compared to the existing models in the 1 mm to 30 cm wavelength range under nominal jovian conditions for a mixture of NH_3 = 0.05%, He = 13.5%, H_2 = 86.45% at a pressure of 2 bar and a temperature of 230 K is given in Fig. 13 and a plot of the percentage change of the new ammonia opacity model from previous models under the same conditions is given in Fig. 14.

8. Radiative transfer simulations of jupiter

A radiative transfer model can be used to simulate the millimeter-wavelength emission spectrum of Jupiter as observed from Earth. By incorporating the new ammonia opacity formalism in

Table 6
The percentage of the measured data points within 2σ uncertainty of the new model in comparison with the existing models.

NH_3 opacity model	1.5–27 GHz measurements	22–40 GHz measurements	75–150 GHz measurements	Total
Berge and Gulkis	53.11	89.2	23.59	45.36
Spilker	70.23	48.4	8.69	45.06
Joiner and Steffes	82.88	84.4	19.84	59.32
Mohammed and Steffes (Ka-band)	57.16	55.2	3.95	36.97
Mohammed and Steffes (W-band)	49.13	86.4	25.07	43.54
Hanley et al.	96.09	85.2	10.46	62.88
This work	95.11	94.8	66.44	84.3

Please cite this article in press as: Devaraj, K., et al. Reconciling the centimeter- and millimeter-wavelength ammonia absorption spectra under jovian conditions: Extensive millimeter-wavelength measurements and a consistent model. Icarus (2011), doi:10.1016/j.icarus.2010.12.010

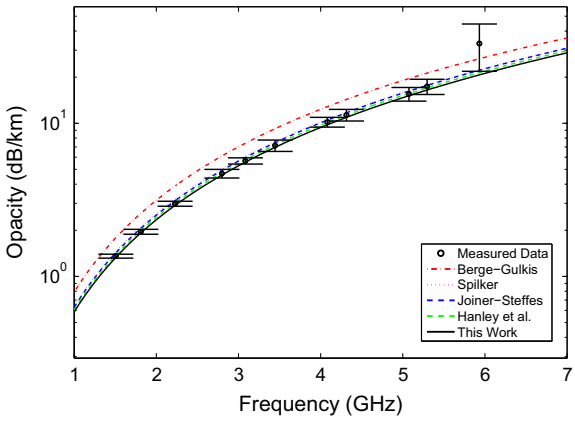

Fig. 5. Opacity data measured by Hanley et al. (2009) using the large cavity resonator for a mixture of NH_3 = 0.93%, He = 13.47%, H_2 = 85.6% at a pressure of 12.073 bar and a temperature of 373.3 K compared to various models. The Spilker and Joiner–Steffes models overlap in this figure.

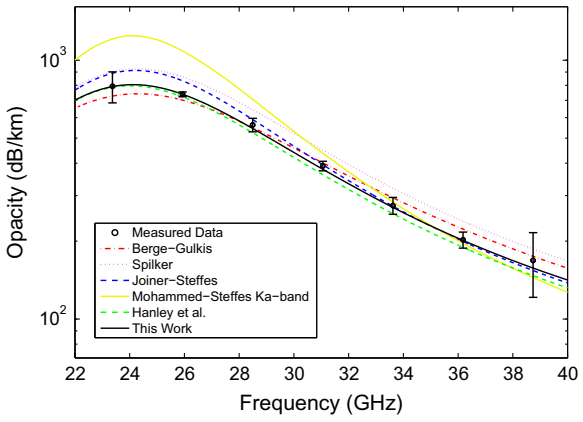

Fig. 6. Opacity data measured by Hanley et al. (2009) using the Ka-band Fabry–Perot resonator for a mixture of NH_3 = 4%, He = 13.06%, H_2 = 82.94% at a pressure of 2 bar and a temperature of 295.3 K compared to various models.

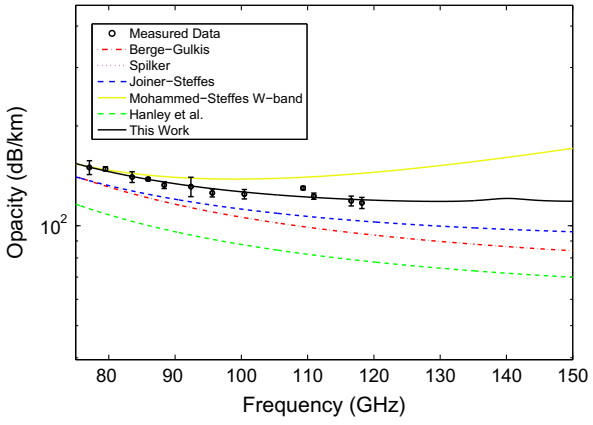

Fig. 7. Opacity data measured using the W-band system for a mixture of NH_3 = 5.06%, He = 12.91%, H_2 = 82.03% at a pressure of 1.943 bar and a temperature of 207.7 K compared to various models.

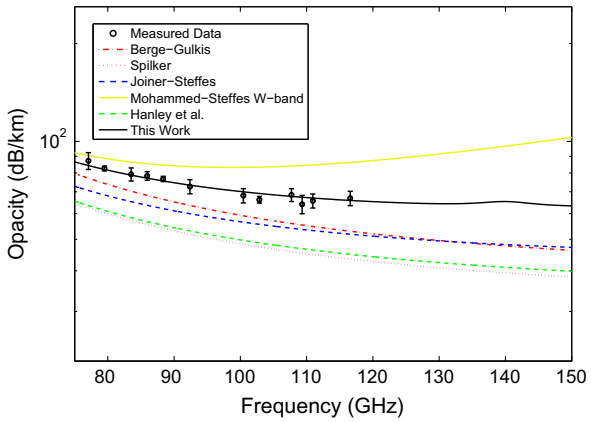

Fig. 8. Opacity data measured using the W-band system for a mixture of NH_3 = 2.14%, He = 13.31%, H_2 = 84.55% at a pressure of 2.766 bar and a temperature of 221.6 K compared to various models.

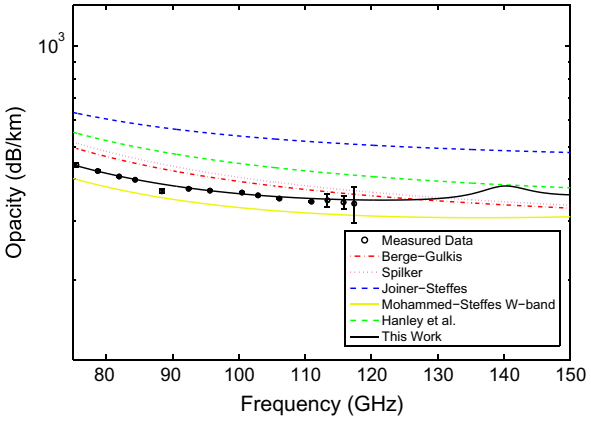

Fig. 9. Opacity data measured using the W-band system for pure ammonia gas at a pressure of 0.505 bar and a temperature of 296.7 K compared to various models.

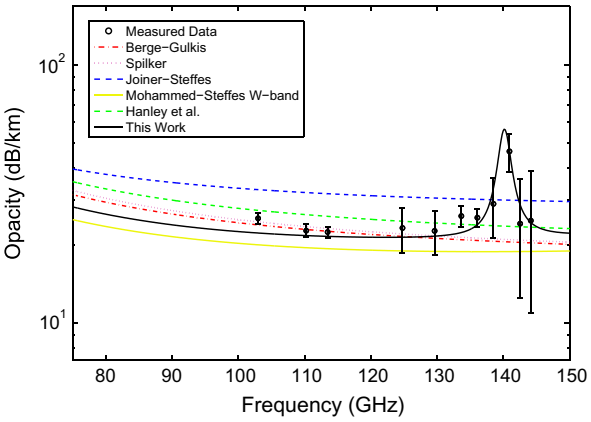

Fig. 10. Opacity data measured using the F-band system for pure ammonia gas at a pressure of 0.124 bar and a temperature of 295.9 K compared to various models.

the radiative transfer calculations of Jupiter, it is possible to analyze the effects of the new formalism on the modeled brightness temperature of the planet. An elliptical-shell, ray-tracing-based, local radiative transfer model (LRTM) used for this analysis was developed by Hoffman et al. (2001) and modified by Karpowicz (2010). The LRTM relies on a thermochemical model (TCM) developed by DeBoer and Steffes (1996) and modified by Karpowicz (2010) to model the distribution and abundances of the constituent elements and the temperature–pressure (*TP*) profile of the atmosphere of Jupiter. The construction begins, in general, from some assumption of the deep abundance of atmospheric

Please cite this article in press as: Devaraj, K., et al. Reconciling the centimeter- and millimeter-wavelength ammonia absorption spectra under jovian conditions: Extensive millimeter-wavelength measurements and a consistent model. Icarus (2011), doi:10.1016/j.icarus.2010.12.010

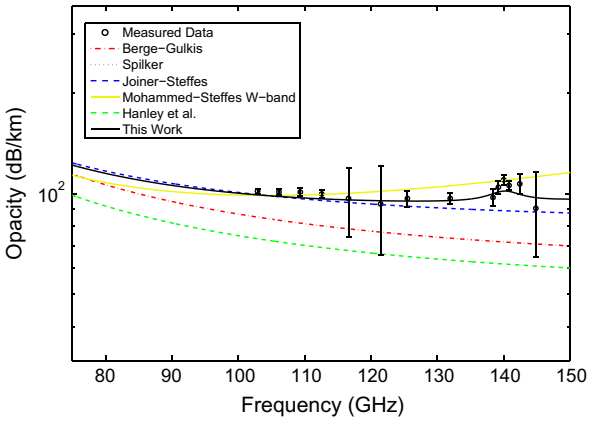

Fig. 11. Opacity data measured using the F-band system for a mixture of NH_3 = 10.89%, He = 12.12%, H_2 = 76.99% at a pressure of 1.089 bar and a temperature of 220.7 K compared to various models.

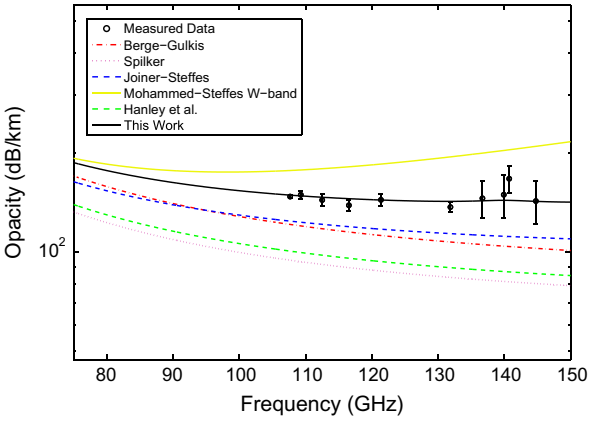

Fig. 12. Opacity data measured using the F-band system for a mixture of NH_3 = 3.41%, He = 13.14%, H_2 = 83.45% at a pressure of 2.791 bar and a temperature of 208.1 K compared to various models.

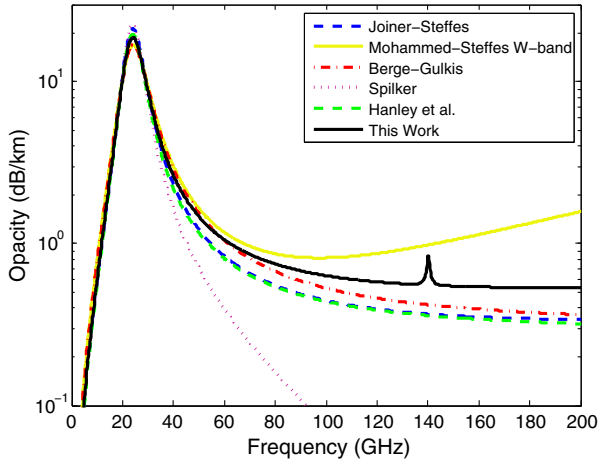

Fig. 13. The opacity computed using the new model compared to the previous models in the 1.5 mm to 30 cm wavelength range under nominal jovian *TP* conditions (for a mixture of NH_3 = 0.05%, He = 13.43%, H_2 = 86.53% at a pressure of 2 bar and a temperature of 230 K).

constituents. The *TP* profile is then computed using a wet-adiabatic extrapolation in discrete layers of pressure, starting at the deepest layer and ending at the 1 bar pressure level. For pressures less than

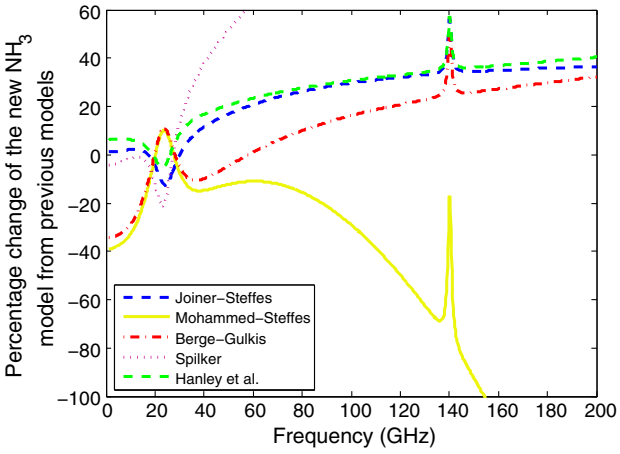

Fig. 14. The percentage change of the new opacity model from previous models for a mixture of NH_3 = 0.05%, He = 13.42%, H_2 = 86.53% at a pressure of 2 bar and a temperature of 230 K.

1 bar, the Voyager radio occultation results summarized in tabular form by Lindal (1992) are used. The assumed mole fraction of various constituents in the deep atmosphere of Jupiter for the LRTM construction are as follows: $X_{He} = 0.1346, X_{H_2O} = 0.0055$, $X_{H_2S} = 66.01$ ppm, $X_{NH_3} = 300$ ppm or 600 ppm, and rest H_2. These abundance values are based on recent studies of the composition of Jupiter (e.g., Atreya et al., 2003). Since the abundance of PH_3 in Jupiter is very small (e.g., Kunde et al., 1982), and because there are no strong absorption lines of PH_3 in the 2–4 mm-wavelength range (e.g., Pickett et al., 1998), it is not included in the LRTM simulations. Two different concentrations of NH_3 are used in the simulations to show the approximate impact of the changes in NH_3 mole fraction on the resulting brightness temperature and do not represent the upper and lower bounds on the established NH_3 concentration in Jupiter. Fig. 15 shows the *TP* profile of Jupiter overlayed with the normalized weighting functions (which indicate the levels that contribute most to the brightness temperature at a particular frequency) at 140.143 GHz.

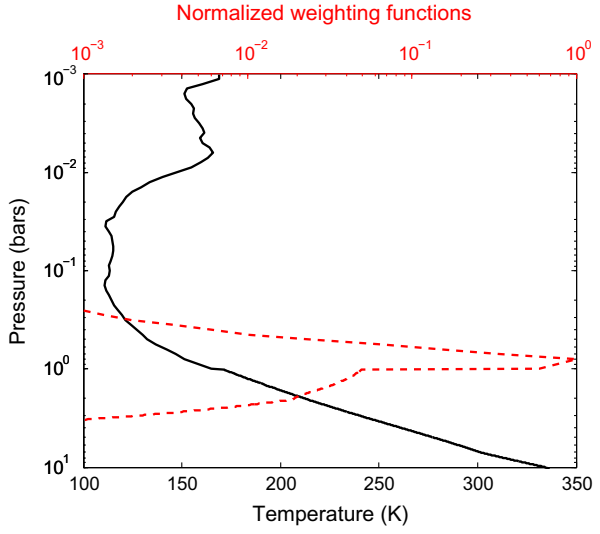

Fig. 15. The temperature–pressure (TP) profile of Jupiter is shown as a black line. The TP profile above the 1-bar level represents the Voyager radio occultation results summarized by Lindal (1992), and the TP profile below the 1-bar level represents the results of a wet-adiabatic extrapolation using the thermochemical model developed by DeBoer and Steffes (1996) and modified by Karpowicz (2010). The normalized weighting functions at 140.14 GHz for 600 ppm NH_3 concentration is shown as a red dashed line. (For interpretation of the references to color in this figure legend, the reader is referred to the web version of this article.)

Please cite this article in press as: Devaraj, K., et al. Reconciling the centimeter- and millimeter-wavelength ammonia absorption spectra under jovian conditions: Extensive millimeter-wavelength measurements and a consistent model. Icarus (2011), doi:10.1016/j.icarus.2010.12.010

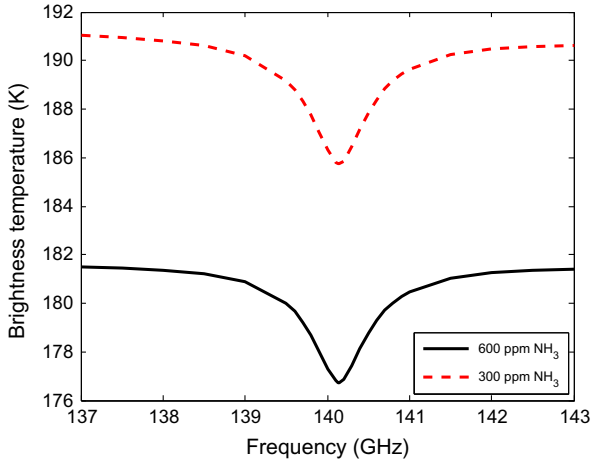

Fig. 16. Predicted disk-averaged brightness temperatures of Jupiter for two different ammonia concentrations.

Once the constituent abundances, temperature, and pressure in each layer has been defined, the absorption of each layer is calculated. The collision induced absorption between H_2–H_2, H_2–He, and H_2–CH_4 are calculated using a model given by Orton et al. (2007). Absorption from NH_3 is computed using the latest formalism described in this paper. Absorption from H_2O is computed using a formalism developed by Karpowicz (2010), and absorption from H_2S is computed using a formalism developed by DeBoer and Steffes (1994). The outgoing electromagnetic radiation exiting the atmosphere of Jupiter at the measurement frequency is predicted by the black body thermal emission of each layer and the absorption of its constituents. The disk-averaged brightness temperature of Jupiter in the 137–143 GHz range for the two NH_3 concentrations is shown in Fig. 16. It can be seen from the figure that the predicted disk-averaged brightness temperature of Jupiter varies by approximately 10 K for the two different ammonia concentration cases indicating that the 2.1 mm-wavelength range is sensitive to the deep ammonia abundance. It can also be seen from the figure that the line center of the 140.14 GHz v_2 roto-vibrational transition of ammonia is at least 5 K darker than the continuum emission. This ammonia line transition in Jupiter can be observed with millimeter-wavelength telescope facilities such as the Institut de Radioastronomie Millimétrique (IRAM).

9. Discussion

Millimeter waves probe the upper and middle tropospheres of jovian planets ($P < 5$ bars) providing unique insights into the atmospheric composition, chemistry, and dynamics of those layers in the planetary atmospheres. Centimeter waves probe the middle and deep atmospheres of jovian planets (pressures up to hundreds of bars) and hence help infer the interior composition and dynamics of the planetary atmospheres. Research into the problem of developing a unified formalism to estimate the centimeter- and millimeter-wavelength opacity spectra of ammonia at the pressures, temperatures, and mixing ratios characteristic of the outer planets has been on-going for more than 30 years since the work by Berge and Gulkis (1976) (see, e.g., Mohammed and Steffes, 2004). This new model can be used to estimate the opacity of ammonia under jovian conditions in the 1–30 cm wavelength range at pressures up to 20 bars and temperatures from 200 to 500 K and in the 1 mm to 1 cm wavelength range at pressures up to 3 bars and temperatures from 200 to 300 K. Various parameters of the model were optimized to fit the centimeter-wavelength data measured at pressures up to 12 bars and temperatures up to 450 K. The model can be used in the centimeter-wavelength range with reasonable certainty at slightly higher pressures and temperatures. However, the model cannot be used for study of the deep interiors of the jovian planets where pressures exceed 20 bars. While the model performance was studied, it was found that the model is very sensitive to changes in the hydrogen- broadening parameter (γ_{H_2}) of the inversion lines. For example, by reducing this parameter by 12% from its current value, the altered model can fit the high pressure data (pressures up to 700 bars) measured by Morris and Parsons (1970) within their uncertainty limits. However, there are other factors that change in the gas mixtures as the pressure is increased such as the deviation from the ideal gas behavior which are not included in the altered model used to match the Morris and Parsons data. Furthermore, some assumptions about the elastic collisions used for most of the lineshape theories are invalid under the high pressure conditions. Additionally, the integrity of the fit to the millimeter-wavelength measurements described in this paper was compromised by altering the model. Hence, the model described in this paper, albeit consistent in the centimeter- and millimeter-wavelength range, can only be used to compute the opacity of ammonia under jovian conditions at pressures up to 20 bars in the 1–30 cm wavelength range and pressures up to 3 bars in the 1 mm to 1 cm wavelength range. Laboratory measurements of the 5–20 cm opacity of ammonia under deep jovian conditions (pressures up to 100 bars and temperatures up to 500 K) are currently being performed by Devaraj and Steffes (2010) using an ultra-high pressure system developed by Karpowicz (2010). These high pressure measurements and the 1.5–27 GHz measurements made by Hanley et al. (2009) will be used to develop a high-pressure centimeter-wavelength model that can be used at pressures up to hundreds of bars under jovian conditions. Since millimeter waves do not penetrate the deep interiors of the jovian planetary atmospheres, the new model is valid for nearly all applications in the millimeter-wavelength range. Furthermore, the new model can also be used in the centimeter-wavelength range under jovian conditions at pressures up to 20 bars.

10. Conclusions

While the initial objective of this research was to better understand the *millimeter-wavelength* opacity of gaseous ammonia under jovian conditions, the results of our laboratory measurements of the opacity of ammonia helped create the most accurate and consistent model to date to represent the 1 mm to 30 cm opacity of ammonia pressure-broadened by hydrogen and helium. The measurements also contribute to the empirical estimation of the self-, hydrogen-, and helium- broadening parameters of the 140.14 GHz v_2 roto-vibrational transition of ammonia for the first time in a laboratory setting. The new model significantly outperforms the other models in the millimeter-wavelength region and performs almost as well as the model developed by Hanley et al. (2009) in the centimeter-wavelength region and can be used for accurate retrievals of ammonia and other constituents in the jovian planetary atmospheres from ground-based and spacecraft-based radio observations. Furthermore, radiative transfer calculations of Jupiter show that the 140.14 GHz v_2 roto-vibrational transition of ammonia is observable using facilities such as the IRAM telescope. Future work will involve the search for the 140.14 GHz v_2 line with the IRAM telescope. Future work will also involve the measurements of the opacity of ammonia in the 5–20 cm wavelength range under deep jovian conditions at pressures up to 100 bars and temperatures up to 500 K, and the development of a high-pressure ammonia opacity model that can work at pressures up to hundreds of bars under jovian conditions.

Please cite this article in press as: Devaraj, K., et al. Reconciling the centimeter- and millimeter-wavelength ammonia absorption spectra under jovian conditions: Extensive millimeter-wavelength measurements and a consistent model. Icarus (2011), doi:10.1016/j.icarus.2010.12.010

Acknowledgments

This work is supported by the NASA Planetary Atmospheres Program under Grant NNG06GF34G. The authors wish to thank Dr. Thomas R. Hanley for his valuable contributions to the Fabry–Perot resonator design and data processing software, and useful discussions about ammonia opacity formalisms.

Appendix A. Supplementary material

Supplementary material associated with this article can be found, in the online version, at doi:10.1016/j.icarus.2010.12.010.

References

Atreya, S., Mahaffy, P., Niemann, H., Wong, M., Owen, T., 2003. Composition and origin of the atmosphere of Jupiter – An update, and implications for the extrasolar giant planets. Planet. Space Sci. 51, 105–112.

Bachet, G., 1973. Etude des elargissements de la raie de rotation a 19 cm^{-1} de NH_3 perturbee par des gaz etrangers comprimes. J. Quant. Spectrosc. Radiat. Trans. 13, 1305–1308.

Belli, S., Buffa, G., Tarrini, O., 1997. On the extension of the Rydberg–Ritz principle to the collisional relaxation of molecular and atomic lines. Chem. Phys. Lett. 193, 277–284.

Belov, S.P., Kazakov, V.P., Krupnov, A.F., Markov, V.N., Mel'nikov, A.A., Skvortsov, V.A., Tret'yakov, M.Y., 1982. The study of microwave pressure linewidths. J. Mol. Spectrosc. 94, 264–282.

Belov, S.P., Krupnov, A.F., Markov, V.N., Mel'nikov, A.A., Skvortsov, V.A., Tret'yakov, M.Y., 1983. Study of microwave pressure lineshifts: Dynamic and isotopic dependences. J. Mol. Spectrosc. 101, 258–270.

Ben-Reuven, A., 1966. Impact broadening of microwave spectra. Phys. Rev. 145, 7–22.

Berge, G.L., Gulkis, S., 1976. Earth-based radio observations of Jupiter: Millimeter to meter wavelengths. In: Gehrels, T. (Ed.), Jupiter: Studies of the Interior, Atmosphere, Magnetosphere, and Satellites. Univ. of Arizona Press, Tuscon, AZ, pp. 621–692.

Bleaney, B., Loubser, J.H.N., 1950. The inversion spectra of NH_3, CH_3C1 and CH_3Br at high pressures. Proc. Phys. Soc., Sect. A. 63, 483–493.

Bleaney, B., Penrose, R.P., 1947. The inversion spectrum of ammonia at centimetre wave-lengths. Proc. R. Soc. A 189, 358–371.

Brown, L.R., Peterson, D.B., 1994. An empirical expression for linewidths of ammonia from far-infrared measurements. J. Mol. Spectrosc. 168, 593–606.

Cleeton, C.E., Williams, N.H., 1934. Electromagnetic waves of 1.1 cm wave-length and the absorption spectrum of ammonia. Phys. Rev. 45, 234–237.

DeBoer, D.R., Steffes, P.G., 1994. Laboratory measurements of the microwave properties of H_2S under simulated jovian conditions with an application to Neptune. Icarus 109, 352–366.

DeBoer, D.R., Steffes, P.G., 1996. Estimates of the tropospheric vertical structure of Neptune based on microwave radiative transfer studies. Icarus 123, 323–335.

Debye, P.J.W., 1929. Polar Molecules. The Chemical Catalog Company Inc., New York.

Devaraj, K., Steffes, P.G., 2011. The Georgia Tech millimeter-wavelength measurement system and some applications to the study of planetary atmospheres. Radio Sci., in press. doi:10.1029/2010rs004433.

Devaraj, K., Steffes, P.G., 2010. Laboratory measurements of microwave properties of ammonia under deep jovian atmospheric conditions. Lunar Planet. Sci. 41. Abstract 1875.

Dowling, T.E., Muhleman, D.O., Berge, G.L., 1987. Aperture synthesis observations of Saturn and its rings at 2.7-mm wavelength. Icarus 70, 506–516.

Dunn, D.E., de Pater, I., Wright, M., Hogerheijde, M.R., Molnar, L.A., 2005. High-quality BIMA-OVRO images of Saturn and its rings at 1.3 and 3 millimeters. Astron. J. 129, 1109–1116.

Griffin, M.J., Orton, G.S., 1993. The near-millimeter brightness temperature spectra of Uranus and Neptune. Icarus 105, 537–547.

Griffin, M.J., Ade, P.A.R., Orton, G.S., Robson, E.I., Gear, W.K., Nolt, I.G., Radostitz, J.V., 1986. Submillimeter and millimeter observations of Jupiter. Icarus 65, 244–256.

Gross, E.P., 1955. Shape of collision-broadened spectral lines. Phys. Rev. 97, 395–403.

Hanley, T.R., Steffes, P.G., 2007. A high-sensitivity laboratory system for measuring the microwave properties of gases under simulated conditions for planetary atmospheres. Radio Sci. 42 (RS6010).

Hanley, T.R., Steffes, P.G., Karpowicz, B.M., 2009. A new model of the hydrogen and helium-broadened microwave opacity of ammonia based on extensive laboratory measurements. Icarus 202, 316–335.

Hoffman, J.P., Steffes, P.G., DeBoer, D.R., 2001. Laboratory measurements of the microwave opacity of phosphine: Opacity formalism and application to the atmospheres of the outer planets. Icarus 152, 172–184.

Joiner, J., Steffes, P.G., 1991. Modeling of Jupiter's millimeter wave emission utilizing laboratory measurements of ammonia (NH_3) opacity. J. Geophys. Res. 96, 17463–17470.

Karpowicz, B.M., 2010. In Search of Water Vapor on Jupiter: Laboratory Measurements of the Microwave Properties of Water Vapor and Simulations of Jupiter's Microwave Emission in Support of the Juno Mission. PhD Dissertation, Georgia Institute of Technology, Atlanta, GA.

Kramer, C., Moreno, R., Greve, A., 2008. Long-term observations of Uranus and Neptune at 90 GHz with IRAM 30 m telescope. Astron. Astrophys. 482, 359–363.

Kunde, V., Hanel, R., Maguire, W., Gautier, D., Baluteau, J.P., Marten, A., 1982. The tropospheric gas composition of Jupiter's north equatorial belt (NH_3, PH_3, CH_3D, GeH_4, H_2O) and the jovian D/H isotopic ratio. Astrophys. J. 263, 443–467.

Levenberg, K., 1944. A method for the solution of certain nonlinear problems in least squares. Quart. Appl. Math. 2, 164–168.

Lindal, G.F., 1992. The atmosphere of Neptune – An analysis of radio occultation data acquired with Voyager 2. Astron. J. 103, 967–982.

Lorentz, H.A., 1906. The width of spectral lines. Proc. Neth. Acad. Arts Sci. 18, 134–150.

Marquardt, D., 1963. An algorithm for least-squares estimation of nonlinear parameters. SIAM J. Appl. Math. 11, 431–441.

Mohammed, P.N., Steffes, P.G., 2003. Laboratory measurements of the K_a-band (7.5 to 9.2 mm) opacity of phosphine (PH_3) and ammonia (NH_3) under simulated conditions for the Cassini-Saturn encounter. Icarus 166, 423–435.

Mohammed, P.N., Steffes, P.G., 2004. Laboratory measurements of the W band (3.2 mm) properties of phosphine (PH_3) and ammonia (NH_3) under simulated conditions for the outer planets. J. Geophys. Res. 109 (E07S13).

Morris, E.C., Parsons, R.W., 1970. Microwave absorption by gas mixtures at pressures upto several hundred bars. I. Experimental technique and results. Aust. J. Phys. 23, 335–349.

Muhleman, D.O., Berge, G.L., 1991. Observations of Mars, Uranus, Neptune, Io, Europa, Ganymede and Callisto at a wavelength of 2.66 mm. Icarus 92, 263–272.

Nethercot, A.H., Klein, J.A., Loubser, J.H.N., Townes, C.H., 1952. Spectroscopy near the boundary between the microwave and infrared regions. Suppl. Nuovo Cimento 9, 358–363.

Orton, G.S., Gustafsson, M., Burgdorf, M., Meadows, V., 2007. Revised ab initio models for H_2–H_2 collision-induced absorption at low temperatures. Icarus 189, 544–549.

Pickett, H.M., Poynter, R.L., Cohen, E.A., Delitsky, M.L., Pearson, J.C., Müller, H.S.P., 1998. Submillimeter, millimeter, and microwave spectral line catalog. J. Quant. Spectrosc. Radiat. Trans. 60, 883–890.

Pine, A.S., Markov, V.N., Buffa, G., Tarrini, O., 1993. N_2, O_2, H_2, Ar and He broadening in the ν_1 band of NH_3. J. Quant. Spectrosc. Radiat. Trans. 50, 337–348.

Poynter, R.L., Kakar, R.K., 1975. The microwave frequencies, line parameters, and spectral constants for $14NH_3$. Astrophys. J. Suppl. Ser. 29, 87–96.

Span, R., 2000. Multiparameter Equations of State. Springer, New York.

Spilker, T.R., 1990. Laboratory Measurements of the Microwave Absorptivity and Refractivity Spectra of Gas Mixtures Applicable to Giant Planet Atmospheres. PhD Dissertation, Stanford University, CA.

Townes, C.H., Schawlow, A.L., 1955. Microwave Spectroscopy. McGraw-Hill, New York.

Ulich, B.L., 1974. Absolute brightness temperature measurements at 2.1-mm wavelength. Icarus 21, 254–261.

Ulich, B.L., 1981. Millimeter-wavelength continuum calibration sources. Astron. J. 86, 1619–1626.

Valdes, F., Welch, W.J., Haber, D., 1982. The jovian ammonia abundance from interferometric observations of limb darkening at 3.4 mm. Icarus 49, 17–26.

Valkenburg, E.P., Derr, V.E., 1966. A high-Q Fabry–Perot interferometer for water vapor absorption measurements in the 100 Gc/s to 300 Gc/s frequency range. Proc. IEEE 54, 493–498.

van der Tak, F., de Pater, I., Silva, A., Millan, R., 1999. Time variability in the radio brightness distribution of Saturn. Icarus 142, 125–147.

Van der Waals, 1873. On the Continuity of the Gaseous and Liquid States. PhD Dissertation, Universiteit Leiden, Leiden, Netherlands.

Van Vleck, J.H., Weisskopf, V.F., 1945. On the shape of collision-broadened lines. Rev. Mod. Phys. 17, 227–236.

von Zahn, U., Hunten, D.M., Lehmacher, G., 1998. Helium in Jupiter's atmosphere: Results from the Galileo probe helium interferometer experiment. J. Geophys. Res. 103, 22815–22829.

Waters, J.W., 1976. Absorption and emission by atmospheric gases. In: Meeks, M.L. (Ed.), Methods of Experimental Physics, vol. 12B. New York Academic Press, New York, NY.

Yu, S., Drouin, B.J., Pearson, J.C., 2010a. Species tag: 17002 Version 5. <http://spec.jpl.nasa.gov/ftp/pub/catalog/doc/d017002.pdf>.

Yu, S., Drouin, B.J., Pearson, J.C., 2010b. Species tag: 17004 Version 5. <http://spec.jpl.nasa.gov/ftp/pub/catalog/doc/d017004.pdf>.

Yu, S. et al., 2010c. Submillimeter-wave and far-infrared spectroscopy of high-J transitions of the ground and $\nu_2 = 1$ states of ammonia. J. Chem. Phys. 133, 174317.